ИНСТИТУТ ЯДЕРНОЙ ФИЗИКИ
им. Г.И. Будкера СО РАН

V.A. Chernov, S.V. Mytnichenko, S.G. Nikitenko

XAFS-LIKE STRUCTURE OF RESONANT RAMAN SCATTERING

BUDKERINP 92-88

НОВОСИБИРСК

XAFS-Like Structure of Resonant Raman Scattering

V.A.Chernov[*], S.V.Mytnichenko[**] and S.G.Nikitenko[*]

Budker Institute of Nuclear Physics

630090, Novosibirsk 90, Russia

ABSTRACT

The KM resonant Raman scattering from a nickel sample has been measured at an energy of incident X-ray photons, of about 120 eV below the K-edge. As far as we know, XAFS-like oscillations have been observed in the scattered spectrum for the first time. The observed spectrum is compared with the XAFS spectrum. The basic differences between these two methods are discussed.

*) Institute of Catalysis.
**) Institute of Solid State Chemistry. Siberian SR Centre at the Budker Institute of Nuclear Physics.
Telex: 133116 ATOM SU; Fax: +7(3832)35-21-63.

INTRODUCTION

The resonant enhancement of inelastic scattering near the atomic absorption edge was experimentally discovered by Sparks in 1974 [1]. He pointed out that the observed inelastic scattering (Resonant Raman Scattering) may be described by the **pA** term in the electron-photon interaction Hamiltonian

$$H = -(e/mc)\mathbf{pA} + (e^2/2mc^2)A^2 \qquad (1)$$

in second-order perturbation theory.

The basic inelastic X-ray scattering theory, including the resonance phenomena, can be found in Ref. [2]. The cross-section of inelastic scattering may be written (the generalized Kramer-Heiseberg formula) as [3]

$$\left(\frac{d^2\sigma}{d\omega\, d\Omega}\right)_{fi} = r_0^2\left(\frac{\omega}{\omega_0}\right)\delta(\omega_0 - E_f + E_i - \omega) \times \left| \langle f|\exp(ikr)|i\rangle(e_0 e^*) + \right.$$

$$\left. + \frac{1}{m}\sum_n \left(\frac{\langle f|pe_0|n\rangle\langle n|pe^*|i\rangle}{E_i - E_n - \omega} + \frac{\langle f|pe^*|n\rangle\langle n|pe_0|i\rangle}{E_i - E_n + \omega_0 + \frac{1}{2}i\Gamma_n}\right)\right|^2 \qquad (2)$$

Here r_0 is the classical electron radius, $\langle i|$, $\langle f|$, $\langle n|$, E_i, E_f, E_n are the ground, final and intermediate states of an

atom and its energies respectively, ω_0, ω are the incident and scattered photon energies, $\mathbf{e}_0$, $\mathbf{e}$ are the complex polarization vectors of the incident and scattered radiation, Γ_n is the total width of the state and $\mathbf{p}$ is the momentum operator. Under certain conditions, if the photon energy ω_0 lies slightly below the absorption edge and the denominator of the resonant term becomes small, it is possible to neglect the first and second terms in eq.2. This is the case of pure RRS without any complications.

According to quantum electrodynamics, RRS may be described as a two stage process (Fig.1). At the first stage, the atom absorbs the incident photon. Then the excited virtual (intermediate) state of the atom disintegrates, with the emission of a new photon and one or few photoelectrons. In the one-electron approximation, the RRS may be classified using core hole states of the atom. For example, for KM RRS the intermediate state of the atom is a state with a hole on the K-shell, and the final state is a state with a hole on the M_{II} or M_{III}-shell. The specific energy levels that are involved in KM RRS process are schematically depicted in Fig.1.

Under the above conditions it is possible to show that the KM RRS cross-section is proportional to the K-edge absorption cross-section [4]

$$\frac{d\sigma}{d\omega} \sim \frac{\sigma_{abc}(\omega_0 - \omega + \Omega_K - \Omega_M)}{(\Omega_K - \Omega_M - \omega)^2 + \Gamma_K^2} \qquad (3)$$

Thus, the RRS spectra should reflect the fine structure of the absorption spectra (XAFS) [5], which is caused by the scattering of the outgoing photoelectron wave from the neighbouring atoms. It was first predicted by Bannet and Freund in their theoretical examination [6] of Sparks' RRS data.

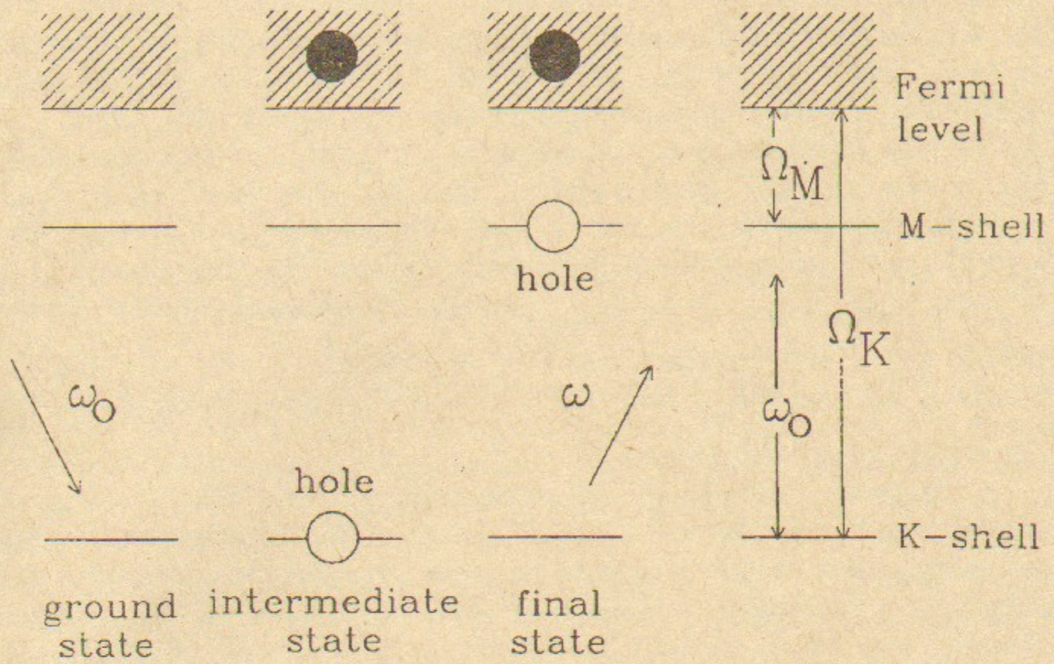

Fig.1. One-electron picture of atomic states involved in the KM RRS process.

The important feature of RRS is as follows. Since the hole creation in the RRS process is off the energy shell, it takes a limited amount of time to detect the fact that the outgoing electron has scattered from its neighbours [4]. Thus, the oscillation amplitude of RRS should be weaker than in absorption spectroscopy. Moreover, the interesting information can be obtained by changing the excitation energy and analyzing the amplitude of XAFS-like oscillations.

Due to the fact that the cross-section of RRS is very small, there is only a sparse number of reported data. As a rule, in order to increase the counting rate, a solid state detector with poor energy resolution is used. However, a few RRS experiments with moderate energy resolution were carried out.

Using monochromatized Cu K_α radiation from a conven-

tional fine focus X-ray tube and a Johann type spectrometer as an analyzer, Suortti and his colleagues [7] obtained the KL RRS spectrum of nickel with an energy resolution of about 15 eV. They observed very weak modulations in the RRS spectrum. These modulations were classified by them as XAFS-like oscillations. According to our point of view, their results are controversial due to the fact that their experimental technique has a few disadvantages. Firstly, the energy resolution was rather poor. Secondly, the energy gap between the $2p_{1/2}$ and $2p_{3/2}$ levels is about a half of the period of XAFS-oscillations for Ni metal. Thus, the superposition of the KL_{II} and KL_{III} spectra reduces strongly the amplitude of oscillations.

Udagawa and Tohji [8] reported the KL RRS spectra of copper and its oxides. Since their main interest was the pre-edge and edge structures, the excitation energy was about 30 eV below the energy of the copper K-edge. Even though the total resolution of their setup was good (6 eV) for the observation of XAFS-like oscillations, no such feature was observed. Apparently, the superposition of the KL_{II} and KL_{III} RRS spectra made difficult to observe XAFS-like oscillations, just as in Ref.[7].

Here we present our preliminary results dealing with the KM RRS of nickel. The main purpose of our study was to obtain the more precise RRS data with good energy resolution (7 eV) and to observe the XAFS-like oscillations of RRS. We have decided to study KM RRS for the following reason. The energy gap between the $3p_{1/2}$ and $3p_{3/2}$ levels is rather small as compared to the period of XAFS oscillations. Though the total cross-section of RRS increases if the excitation energy approaches the energy of the absorption edge, the differential cross-section decreases very quickly as the energy of the scattered photon decreases. That is why our excitation energy was about 120 eV below the energy of the nickel K-edge.

EXPERIMENTAL

The RRS data were obtained at beamline 5 of the Siberian SR Centre at the Institute of Nuclear Physics. The layout of the experimental device is shown in Fig.2. The white beam from the 2T wiggler of the VEPP-3 storage ring with the current 120-70 mA is monochromatized and simultaneously focused in horizontal plane by an asymmetrically cut (8°) and cylindrically bent triangular Ge (111) crystal [9]. The energy resolution was better than 5 eV at an excitation energy of 8.21 keV. The incident and reflected beam focal distances are 17.5 m and 4.5 m, respectively. The focal spot section was about 0.8 mm in width and 10.0 mm in height.

The measurements were obtained on a nickel polycrystalline foil of 100 μm thickness. In order to eliminate

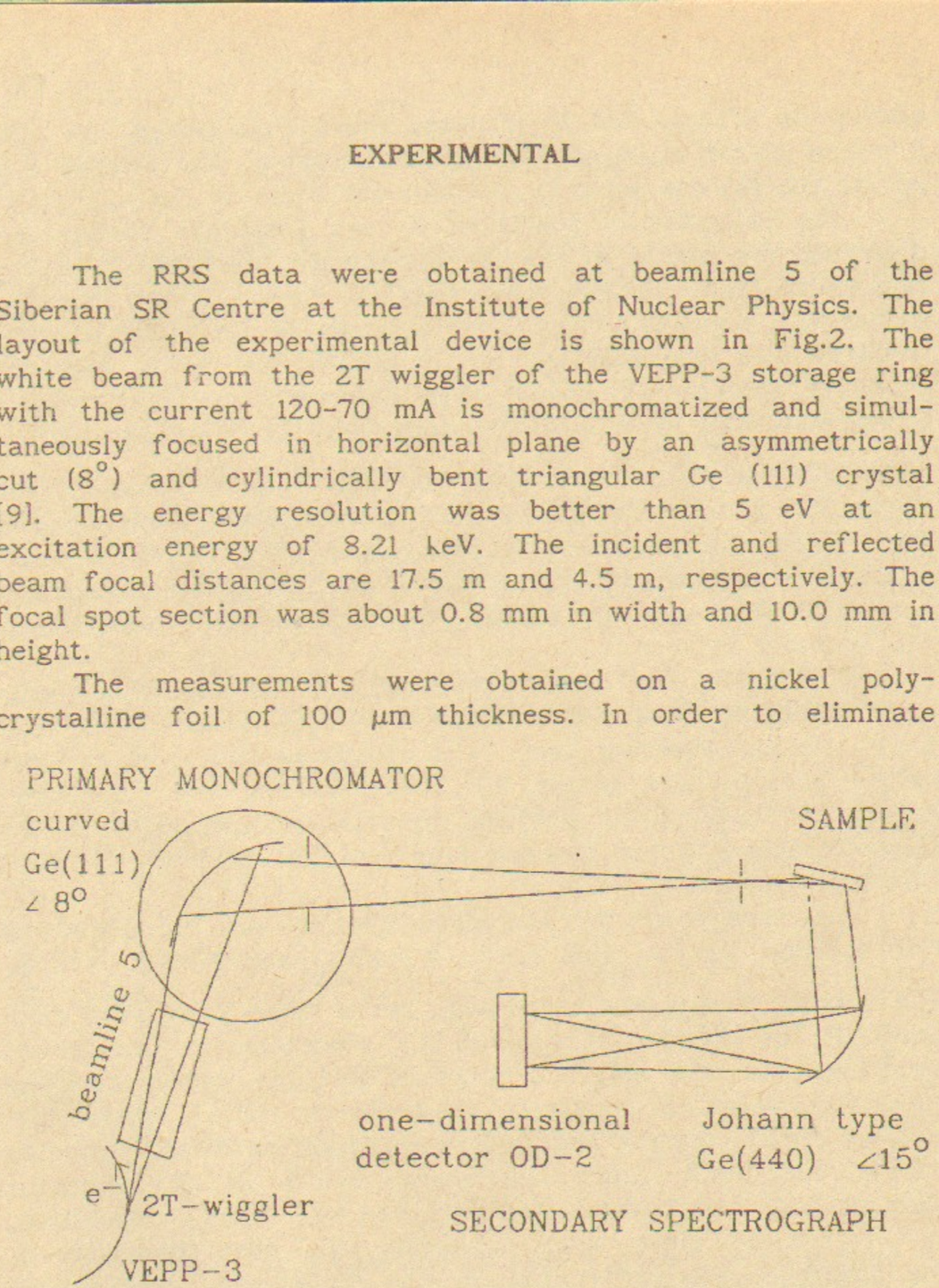

Fig.2. The layout of the experimental device.

absorption effects and to increase the sample image on the Rowland circle of a secondary spectrometer, the sample was set at the oblique angle to the incident beam.

The inelastically scattered X-rays from the sample are dispersed by means of an asymmetrically cut (15°) and cylindrically bent Johann-type Ge(440) crystal. The bending radius was about 600 mm. The spectrum of the radiation distributed over the Rowland circle is analyzed by a position-sensitive detector OD-2 [10]. The detector was filled with a mixture of 80% Xe + 20% CO_2 under 250 kPa (2.5 atm) pressure. The detection efficiency for the 8 keV radiation was about 80% and the spatial resolution was better than 200 μm. The differential nonlinearity was about 2%. For the present experimental geometry, one channel of the spectrum corresponded to 0.85 eV. The energy resolution of the spectrometer was about 4 eV.

To obtain the linear polarization, the incident beam was collimated down to a height of 5 mm. In order to suppress the non-resonant term, the scattering angle of the detected photons was nearly 90°. Nevertheless, the depolarization of the incident photons due to the instability of the electron beam in the storage ring had not allowed to fulfil this task completely.

The energy of the scattered X-rays was calibrated by fluorescence Cu $K\alpha_{1,2}$, W $L\alpha_{1,2}$, Ta $L\alpha_{1,2}$ and Ni $K\beta_{1,3}$ lines. The overall energy resolution was better than 7 eV. The dark noise of the detector was about 0.1 counts/s, the background counting rate was about 2 counts/s and the useful counting rate was about 5 counts/s. In order to obtain good statistics ($5 \cdot 10^3$ counts/channel) the spectrum was collected during one week. Since the energy width of the detector channel was considerably smaller than the energy resolution, the statistical error was negligible and the distortion of the spectrum was determined by the differential nonlinearity of the detector only.

RESULTS AND DISCUSSION

The nickel KM RRS spectrum obtained is shown in Fig.3. For comparison with the experimental spectrum the normalized absorption spectrum is also shown. The last spectrum was prepared using the absorption cross-section of the K-shell, according to eq.(3). The convolution with the resolution function was made. Since the energy gap between the $3p_{1/2}$ and $3p_{3/2}$ states is small (~2 eV), the multiplet-splitting effect was neglected.

First of all, the RRS spectrum obtained indicates the existence of oscillations. The experimental data reproduce oscillations of the absorption spectrum on the low energy

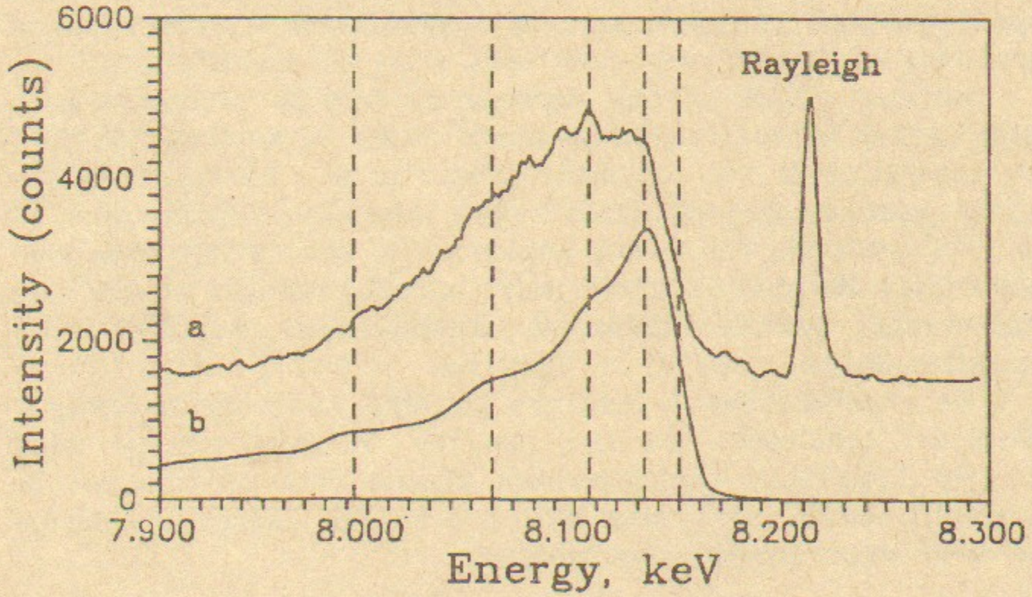

(a) K–M Resonant Raman Scattering of nickel
(b) Normalized Absorption K–edge of nickel

Fig.3. Experimental resonant Raman spectrum (upper curve) of nickel and the normalized K-edge absorption spectrum (bottom curve).

side (EXAFS region). The oscillation amplitude of RRS is weaker according to Ref.[4].

On the other hand, the discrepancy of the measured and calculated data is evident in the region near the KM RRS threshold. This region is analogous to the X-ray Absorption Near Edge Structure (XANES) in absorption spectroscopy. Here we want only to briefly discuss the possible sources of this discrepancy.

The interference of resonant and non-resonant scattering is a possible source of this discrepancy. Though the non-resonant scattering was suppressed due to the polarization condition, the beam instability did not allow to do this completely. According to our assessment, the value of the non-resonant amplitude may be few percents of the resonant amplitude. In contrast with the Compton scattering of valence electrons, which can not give any contribution to the interference effect due to the fact that the final state should be with the hole on the M-shell, the Compton-Raman scattering of M-electrons interferes with the KM RRS.

Another origin of the discrepancy may be connected with many-body effects. The influence of these effects on the RRS and absorption is not the same. Nozieres and Abrahams pointed out that many-body effects give rise to modifications of the RRS spectrum which are analogous to soft X-ray edge singularities. Moreover, many-body effects should cause an interference between different intermediate localized core hole sites [11].

We are planning to continue the RRS experiments using a 100-poles undulator beamline at the VEPP-4 storage ring [12]. We hope that the superhigh photon flux of this source allows to obtain RRS data with more high energy resolution and clear experimental conditions.

Acknowledgements. The authors are very grateful to the SSRC staff and its head G.N.Kulipanov for the assistance in preparing of this work.

REFERENCES

1. *C.J.Sparks.* Jr. Phys. Rev. Lett. 33, 262 (1974).
2. *T.Aberg, J.Tulkki.* In: Atomic Inner-Shell Physics, edited by B.Crasemann, Plenum, New York (1985).
3. *J.Tulkki, T.Aberg.* J. Phys. B15, L435 (1982).
4. *P.Eisenberger, P.M.Platzman, H.Winick.* Phys. Rev. B13, 2377 (1976).
5. XAFS is a general terminology for X-ray absorption spectroscopy including extended (EXAFS) and near-edge structure (XANES). The XAFS theory, as well as examples of applications, can be found in: eds. D.C.Koningsberger and R.Prins, X-ray Absorption, John Wiley & Sons (1988).
6. *Y.Bannet, I.Freund.* Phys. Rev. Lett. 34, 372 (1975).
7. *P.Suortti, V.Etelaniemi, K.Hamalainen, S.Manninen.* J. Phys. C9, 831 (1987).
8. *Y.Udagawa, K.Tohji.*Chem. Phys. Lett. 148, 101 (1988).
9. *A.N.Popov et al.* Nucl. Instrum. and Methods, A282, 510 (1989).
10. *V.M.Aultchenko et al.* Nucl. Instrum. and Methods, 208, 443 (1983).
11. *P.Nozieres, E.Abrahams.* Phys. Rev. B10, 3099 (1974).
12. *V.A.Chernov et al.* X-ray Raman Scattering Station at 100-poles Undulator Beamline at VEPP-4 Storage Ring, abstract on ICAS (1992).

V.A. Chernov, S.V. Mytnichenko, S.G. Nikitenko

XAFS-Like Structure of Resonant Raman Scattering

В.А. Чернов, С.В. Мытниченко, С.Г. Никитенко

Подобная XAFS структура резонантного рамановского рассеяния

ИЯФ 92-88

Ответственный за выпуск С.Г. Попов

Работа поступила 22 ноября 1992 г.
Подписано в печать 22.XI. 1992 г.
Формат бумаги 60×90 1/16 Объем 1,1 печ.л., 0,9 уч.-изд.л.
Тираж 150 экз. Бесплатно. Заказ N 88

Обработано на IBM PC и отпечатано
на ротапринте ИЯФ им. Г.И. Будкера СО РАН,
Новосибирск, 630090, пр. академика Лаврентьева, 11.